RSC Pharmaceutics

ROYAL SOCIETY OF CHEMISTRY

PAPER

Published on 18 September 2026

Cite this: DOI: 10.1039/d6pm00307a

Effect of hydroxypropyl cellulose on the stability and oral absorption of glibenclamide amorphous solid dispersions

Stiliyan Kolev,[a] Vladimir Petkov,[a] Edmont Stoyanov[b] and Zahari Vinarov *[a]

Polymers are widely used in amorphous solid dispersions of poorly water-soluble drugs to provide solid-state and supersaturation stability. While low-molecular-weight hydroxypropyl cellulose polymers usually provide better formulation stability, their effect on high-drug-load formulations is still unclear. Whether spray-dried formulations which sustain supersaturated solutions *in vitro* can increase oral absorption *in vivo* also remains to be verified. Thus, we investigated the effect of the molecular weight of hydroxypropyl cellulose polymers on solid-state stability, dissolution, supersaturation stability and absorption of glibenclamide. Amorphous drug formulations were prepared by spray drying and solvent casting. Solid-state analysis was performed using polarised light microscopy (PLM), differential scanning calorimetry, and wide-angle X-ray diffraction (WAXS). Dissolution was studied in porcine bile extract-based media at fasted- and fed-state conditions. *In situ* rat perfusion was used to assess intestinal absorption. All formulations remained amorphous by PLM and WAXS up to 100 days under ambient storage conditions. Under accelerated stability test conditions, however, lower-molecular-weight polymers consistently provided superior stability, most likely due to improved drug–polymer mixing. Dissolution studies revealed that low-molecular-weight hydroxypropyl cellulose polymers stabilised supersaturated solutions for up to 120 min. *In situ* rat perfusion showed much higher intestinal absorption compared to the crystalline reference. The present study shows that lower-molecular-weight HPCs enhance the performance of high-drug-load ASDs, providing high solid-state and supersaturation stability, as well as significantly improving intestinal absorption.

Received 23rd June 2026,
Accepted 15th September 2026

DOI: 10.1039/d6pm00307a

rsc.li/RSCPharma

1. Introduction

Amorphous solid dispersions (ASDs) are a widely used strategy to improve the oral bioavailability of poorly water-soluble drugs. ASDs act by generating metastable supersaturated solutions which provide high drug concentration gradients across the epithelium of the small intestine, thus enhancing oral absorption.[1–3]

Polymers play a crucial role in ASD formulations as they stabilise the amorphous state of the drug during storage and provide kinetic stabilisation of the supersaturated solution generated upon dissolution.[4,5] However, the ability of the polymer to provide both solid-state and supersaturation stability depends on its physicochemical characteristics, including molecular weight and drug–polymer interactions.[6,7] Polymer molecular weight is a particularly interesting characteristic that can govern drug mobility, drug–polymer miscibility and drug–polymer interactions.[8–10]

The effect of the molecular weight of the polymer on stability and dissolution performance has been studied extensively for polyvinylpyrrolidone (PVP), which provides superior solid-state and supersaturation stability at higher molecular weight.[9–11] This is commonly attributed to the reduced molecular mobility and higher glass transition temperature (T_g) associated with the higher molecular weight polymers.

Hydroxypropyl cellulose (HPC) has emerged as a particularly interesting polymer for ASD development, due to its high aqueous solubility, thermoplasticity and surface activity.[12] However, recent studies with HPC polymers revealed different trends compared to PVP, and a more complex picture. Sarode *et al.* demonstrated the potential of the low-molecular-weight HPC-SSL to stabilise felodipine ASDs and enhance drug dissolution performance.[13] It was also demonstrated that the HPC ASDs outperform PVP-VA, showing superior dissolution performance and comparable solid-state stability at room temperature. Luebbert *et al.* studied the long-term stability and phase separation of HPC-based ASDs produced by spray

[a]*Department of Chemical and Pharmaceutical Engineering, Faculty of Chemistry and Pharmacy, Sofia University, 1 James Bourchier Avenue, 1164 Sofia, Bulgaria. E-mail: zv@lcpe.uni-sofia.bg*
[b]*Nisso Chemical Europe GmbH, Berliner Allee 42, 40212 Düsseldorf, Germany*

drying and showed superior stability for the lower-molecular-weight HPCs (especially HPC-UL) at low drug loads.[8] Other studies of HPC binary and ternary mixtures showed that lower-molecular-weight polymer grades provide easier processing in the context of melt extrusion of celecoxib and efavirenz[14,15] and improved the dissolution of curcumin ternary mixtures with sodium dodecyl sulfate.[16]

In our previous work, we studied the mechanisms of dissolution and crystallisation in biorelevant media of spray-dried amorphous glibenclamide (GLB) formulations stabilised by HPC with different molecular weights.[17] Our results showed that aqueous GLB concentrations are governed by the competition between dissolution and crystallisation, and factors such as drug ionisation, wetting, solubilisation and polymer molecular weight determine which will be the predominating process. Mechanistic experiments showed that the amorphous GLB crystallises following a solid-state transition mechanism, in which crystallisation starts on the surface of the amorphous particles. HPC polymers inhibited this process *via* surface adsorption, and lower-molecular-weight polymers showed superior crystallisation inhibition, most probably due to faster surface adsorption.

Overall, the literature data show that HPC can be used in the formulation and stabilisation of amorphous drug formulations with sustained supersaturation during dissolution. However, data for amorphisation and long-term stability of high-drug-load binary drug–HPC mixtures obtained by spray drying or melt extrusion (which are relevant to industrial settings) remain very limited. Our group[17] and Luebbert *et al.*[8] studied the stability of spray-dried formulations with high drug load (25 and 30 wt%, respectively) of glibenclamide (GLB), fenofibrate or itraconazole for up to 4 months, but failed to discriminate between the studied HPC grades, which showed similar performance. Hence, there is a specific gap in understanding the effect of HPC molecular weight on ASD stability of formulations of particular relevance to the pharmaceutical industry: high-drug-load ASDs obtained by spray drying or melt extrusion.

Another important question for pharmaceutical development is whether the generated high aqueous drug concentrations can actually translate into improved bioavailability *in vivo*. However, only a few studies have addressed this challenge, showing that ASDs based on low-molecular-weight HPC improve the oral bioavailability of nobiletin and itraconazole in rats.[18,19] While one of the studies used melt extrusion, which is an industrially relevant technique, the use of spray drying – the other common method for commercial preparation of ASDs – has not yet been studied.

The current study aims to determine the effect of HPC molecular weight on the solid-state stability of high-drug-load formulations (25% GLB) by conducting accelerated stability tests to differentiate between different polymer grades. In addition, the amorphous stability of the spray-dried powders was compared with that of solvent-cast films, which require very small amounts of material and are easy to prepare and evaluate for crystallisation. Finally, following characterization of the dissolution and supersaturation behaviour of the prepared ASDs, their effect on intestinal absorption was studied by the single-pass rat perfusion method with mesenteric vein blood collection.

2. Materials and methods

2.1. Materials

The experiments were performed using GLB (M_w = 494 g mol^{-1}, pK_a = 5.6) as a model poorly water-soluble drug (99%, TCI). A range of HPC polymers provided by Nisso Chemical Europe GmbH were studied including HPC-UL (20 kDa), HPC-SSL (40 kDa), HPC-L (140 kDa) and HPC-M (700 kDa). Dichloromethane (99.8%, Sigma-Aldrich) and methanol (99.9%, Carlo Erba) were used to prepare the solutions for spray drying. For the preparation of HPLC mobile phases, acetonitrile (99.9%, Carlo Erba) and trifluoroacetic acid (99.9%, Sigma-Aldrich) were used. The reagents used to prepare the dissolution media included hydrochloric acid (1 M, Chem-Lab NV), NaCl (99%, Sigma-Aldrich), NaOH (98%, Fluka), and $NaH_2PO_4{\cdot}H_2O$ (99%, Supelco). Porcine bile extract (Sigma) was used as a source of bile salts.

2.2. Methods

2.2.1. Spray drying. GLB and HPC were dissolved in a dichloromethane and methanol mixture (80 : 20 v/v) to obtain a 5 w/v% solution at a 1 : 3 drug-to-polymer weight ratio (25 wt% drug load). When HPC-M was used, the total dissolved solids were reduced to 2.5 w/v% due to the high viscosity of the 5 w/v% solution. The solution was then spray-dried using Büchi mini B-290 spray dryer. The apparatus was set to the following parameters: inlet temperature: 50 °C; outlet temperature: 35 °C; aspirator: 70%; feed flow rate: 10 mL min^{-1}; rotameter gas flow (Q-flow): 30 mm, equal to a gas flow rate of 357 L h^{-1} with a pressure drop of 0.23 bar and actual volume flow (at standard temperature and pressure) of 439 L h^{-1}. The drying gas used was nitrogen (99.99%). Typically, a volume of 50 mL organic solvent solution was spray-dried and ≈1.75 g of solid material was obtained on average (yield of ≈70%). The resulting spray-dried powders (SDPs) were placed under vacuum for 24 h to remove any residual solvent. Finally, the SDPs were kept as described below (section 2.2.3).

2.2.2. Solvent-cast amorphisation protocol. GLB and HPC were dissolved in a dichloromethane and methanol mixture (80 : 20 v/v) to obtain a 5 w/v% solution at a 1 : 3 drug-to-polymer weight ratio. When HPC-M was used, the total dissolved solids were reduced to 2.5 w/v%. 1 μL of the drug–polymer solution was pipetted onto the surface of a microscope slide heated to 100 °C by a Nahita thermoblock Mini T, forming an amorphous or crystalline film. All samples were prepared in triplicate and stored under ambient or accelerated conditions, as described in section 2.2.3.

2.2.3. Stability studies. The physical stability of both SDPs and solvent-cast samples was studied under different storage conditions. The samples were stored in closed, non-hermeti-

cally sealed containers under both storage regimes (1) a desiccator filled with silica (T = 23 °C, relative humidity = 25%) or (2) climate chamber under accelerated conditions (T = 40 °C, relative humidity = 70%). Accelerated conditions were ensured by using a climate chamber Binder KBF-S at 40 °C and relative humidity of 70%. Accelerated stability tests were defined in accordance with ICH guidelines. Considering the T_g of GLB measured in the current study (T_g = 64 °C, see Fig. S7 and S8 in the SI), calculation of the nominal dry-state T/T_g ratio shows T/T_g = 0.93 and 0.88 at T = 40 and 23 °C, respectively. Hence, storage was below, but relatively close to T_g, without accounting for any water plasticization effects at accelerated conditions, which could make the effective T/T_g ratio even higher than 0.93 and potentially bring the system closer to or even above its moisture-conditioned T_g. Solvent-cast films were stored under the same conditions, but in a container open to the atmosphere in the climate chamber.

The solid state of the samples was periodically characterised using a combination of techniques: polarised light microscopy (PLM), differential scanning calorimetry (DSC) and wide-angle X-ray diffraction (WAXS) for the SDPs and PLM for the solvent-cast samples.

2.2.4. Polarised light microscopy. Samples were observed under polarised light using an AxioImager.M2m microscope (Zeiss, Germany) in transmitted, cross-polarised white light passed through a λ-compensator plate. The λ-compensator plate was placed between the sample and the analyser at a 45° angle with respect to both the analyser and polariser. Before imaging, SDPs were first placed on top of a microscope slide. Solvent-cast films were imaged directly, as they were prepared on a microscope slide to begin with.

The quantitative determination of the percentage of crystallised surface in the solvent-cast films was performed using ImageJ software. The area of the total sample and crystalline regions were determined and the percent crystalline surface was calculated using the formula below.

$$\%\,\text{Crystalline surface} = \frac{\text{Crystalline surface area}}{\text{Total surface area}} \times 100$$

To assess the solid state of undissolved material during dissolution, samples were taken from the dissolution media and centrifuged (20 000*g*, 37 °C, after 60, 90 and 120 min) to obtain sediments, which were then placed on a microscope slide and observed.

2.2.5. Differential scanning calorimetry. DSC measurements were performed using a Discovery 250 (TA Instruments, USA). The sample was weighed and then hermetically sealed in an aluminium pan. An empty pan was used as a reference. The two pans were placed on the two thermocouples inside the heating chamber of the apparatus. The heating protocol was set as a temperature ramp from 30 °C to 190 °C at 10 °C min^{-1}, while measuring the normalised heat flow as mW g^{-1}.

2.2.5.1. Modulated differential scanning calorimetry. Modulated DSC was used to determine the glass-transition temperature of the amorphous materials. The measurements were performed using a Discovery 250 (TA Instruments, USA). The sample was weighed and then hermetically sealed in an aluminium pan. An empty pan was used as a reference. The two pans were placed on the two thermocouples inside the heating chamber of the apparatus. Modulation amplitude was set to ± 0.21 °C and modulation period to 40 s. The heating protocol was set as a temperature ramp from 30 °C to 190 °C at 2 °C min^{-1} with 5 min isothermal step in the beginning at 30 °C.

2.2.6. Wide-angle X-ray diffraction. Measurements were performed using the XEUSS 3.0 SAXS/WAXS system (Xenocs, Sassenage, France) equipped with a CuKα X-ray source (λ = 0.154 nm, Xeuss 3.0 UHR Dual Source Mo/Cu) and an Eiger2 4M detector (Dectris Ltd, Baden Daettwil, Switzerland) with slit collimation. The system operated at 50 kV and 0.6 mA, with a sample-to-detector distance of 300 mm, enabling a q-range of 0.03–1.5 $Å^{-1}$. Data acquisition time was set to 20 min.

The solid-state detector captured 2D images where all scattering vectors (angles) within the q-range corresponded to specific detector pixels. Consequently, the exposure time was uniform across all studied angles, as scattering data was collected simultaneously. Samples were enclosed in 2.5 mm diameter metal O-rings, sealed with two Kapton windows (12.5 μm thickness). Scattered intensity was normalised to the incident intensity and corrected for background scattering from the empty sample holder. Absolute scale calibration was applied, and all measurements were conducted at an ambient temperature of approximately 20 °C.

2.2.7. Dissolution studies. The experiments were performed in 10 mL glass bottles placed on Eppendorf ThermoMixer C set at 400 rpm and T = 37 °C. SDP corresponding to 5 mg of GLB was added to 5 mL dissolution media.

The buffer solution was composed of 106 mM NaCl, 29 mM NaH_2PO_4 and the required amount of NaOH to achieve pH = 6.5. Porcine bile extract was added to the buffer medium as a source of bile salts, yielding a final bile salt concentration of 3 or 10 mM. The bile components were pre-dissolved in the buffer at 37 °C under constant stirring for 30 min.

Samples for analysis were taken after 10, 30, 60, 90 and 120 min with a pre-heated syringe and were centrifuged (Sigma 1-16K, Sigma Zentrifugen) at 20 000*g* at T = 37 °C for 5 min. The supernatants were diluted tenfold (1 : 9) with methanol and analysed by HPLC.

2.2.8. HPLC analysis. GLB concentrations in the dissolution media were determined using a Shimadzu HPLC system, equipped with LC-40D X 3 solvent delivery module, autosampler (SIL-40C X3) and a diode array detector (SPD-M40). Chromatographic separation was performed using Waters X-bridge (150 mm × 4.6 mm, 3.5 μm particle size with column guard VanGard (Waters), 3.9 mm × 5 mm-C18, 3.5 μm). The mobile phase consisted of ACN and water with 0.1% TFA at a 60 : 40 v/v ratio under isocratic conditions. The flow rate was set to 1 mL min^{-1}, the injection volume to 5 μL and column temperature to 40 °C. The specific absorption at 230 nm was used to quantify the GLB in the samples. A calibration curve for glibenclamide ($R^2 \geq 0.9998$) was prepared by appropriate dilutions of GLB stock solution in methanol–water.

2.2.9. *In situ* rat perfusion. Single-pass *in situ* rat perfusion was performed following the general approach described by Stappaerts *et al.*[20] Animals with weight between 200 and 300 g were obtained from Experimental and Breeding Facility for Laboratory Animals at the Institute of Neurobiology – Bulgarian Academy of Sciences. Drug intestinal absorption was quantified by collecting blood from the mesenteric vein connected to the perfused small intestinal segment. Hence, the measured drug concentrations reflected drug intestinal absorption without the influence of first-pass metabolism or excretion. The technical procedures are briefly described below.

SDP corresponding to 100 mg of GLB was added to 100 mL of dissolution medium composed of 106 mM NaCl, 29 mM NaH_2PO_4, and porcine bile extract equivalent to 10 mM bile salts (pH 6.5). The mixture was placed on a magnetic stirrer with a water bath at 37 °C and stirred at 400 rpm. After 30 min, the entire dissolution medium was transferred into centrifuge tubes and centrifuged at 20 000*g* for 5 min at 37 °C to remove the undissolved solids. The obtained supernatant was separated and used for the *in situ* rat perfusion studies. Samples of the supernatant were collected both before and after the *in situ* perfusion to quantify the concentration of GLB and verify that no drug precipitation had occurred.

Additionally, the following solutions were prepared prior to the experiment: the transport medium, consisting of Hank's buffered saline solution supplemented with 10 mM HEPES buffer and adjusted to pH 7.4 using 2 N NaOH (0.5 L); a concentrated heparin solution of 1000 U mL^{-1} (4 mL); a diluted heparin solution of 50 U mL^{-1} (40 mL), corresponding to a 20× dilution of the concentrated solution; and an anaesthesia mixture (KEX) containing ketamine (50 mg mL^{-1}, mixed 1 : 2 with xylazine at 5 mg mL^{-1}, 1 : 4) in water.

Procedures are described in the SI. Briefly, two male Wistar rats were used, one as a blood donor and one as the recipient. Donor blood was collected after heparinisation, diluted, and prepared for infusion, while the recipient rat was anaesthetised, temperature-controlled, and surgically prepared. The jugular vein was cannulated for heparin and blood administration, the abdomen was opened, and a selected small-intestinal segment was externalised, flushed, cannulated, and equilibrated with transport medium. The mesenteric vein connected to the same segment was then cannulated carefully to allow venous blood collection from the perfused intestinal segment. The test perfusion solution was introduced into the intestinal lumen at a defined flow rate of 1 mL min^{-1}, while donor blood was infused systemically at 0.33 mL min^{-1} and blood samples were collected at 5-minute intervals. Plasma was later separated and analysed for drug concentrations. At the end of the experiment, the animal was euthanised, and the perfused intestinal segment length was measured.

Prior to blood collection, empty microcentrifuge tubes intended for sample collection were weighed. Blood samples were collected at 5 min intervals during the perfusion experiment. After each sampling, the filled tubes were weighed again to determine the amount of collected blood. The tubes were then centrifuged to separate the plasma fraction. Following centrifugation, plasma was carefully transferred into clean tubes, which were subsequently reweighed.

If the samples were not analysed immediately, plasma was stored in a freezer at −18 °C until further analysis. Prior to analysis, frozen samples were allowed to equilibrate to room temperature and, if necessary, gently vortexed to ensure homogeneity. For protein precipitation, 100 μL of plasma was added to 400 μL of acetonitrile (ACN). The mixture was vortexed for several seconds to achieve complete mixing, then centrifuged at 20 000*g* for 5 min. The resulting supernatant was carefully transferred into HPLC vials and analysed as described in section 2.2.8.

All experimental procedures involving animals were conducted in compliance with Directive 2010/63/EU on the protection of animals used for scientific purposes and were approved by the Bulgarian Food Safety Agency (BFSA) under license No. 451/13.10.2025. Male Wistar rats were housed under standard conditions with free access to food and water prior to the experiments, and all efforts were made to minimize animal suffering. This study is reported in accordance with the ARRIVE 2.0 guidelines.

3. Experimental results

3.1. Solid-state stability

The physical stability of ASDs is a critical factor that determines their suitability for manufacturing. Although the amorphous state offers improved solubility and dissolution rate, it is thermodynamically unstable and prone to crystallisation. The rational choice of a polymeric carrier is essential for the long-term stability. Apart from the chemical structure of the polymer, other structural characteristics such as molecular weight can also influence the solid-state stability of ASDs.

In the present study, ASDs of GLB and HPC polymers with varying molecular weights (UL-18 kDa, SSL-40 kDa, L-140 kDa and M-700 kDa) were prepared by spray drying and solvent casting. Stability studies were conducted under two storage conditions: ambient, at low temperature (23 °C) and average humidity (RH = 25%), and accelerated, at high temperature (40 °C) and high humidity (RH = 70%). The solid state of the samples upon storage was characterised by a combination of techniques including PLM, DSC and WAXS.

3.1.1. Stability of SDPs

3.1.1.1. PLM observations. The PLM observations of the SDPs stored under ambient conditions showed no signs of crystallisation in any of the studied systems even after 100 days of storage (Fig. 1). The SDPs prepared with HPC-M exhibited some birefringent particles immediately after preparation (indicating incomplete amorphisation) but no progressive crystallisation.

Under accelerated conditions, the samples with HPC-L, HPC-M, and, to a much lesser extent, HPC-SSL showed birefringent particles after 21 days although the material was still mostly composed of amorphous particles. This effect was least

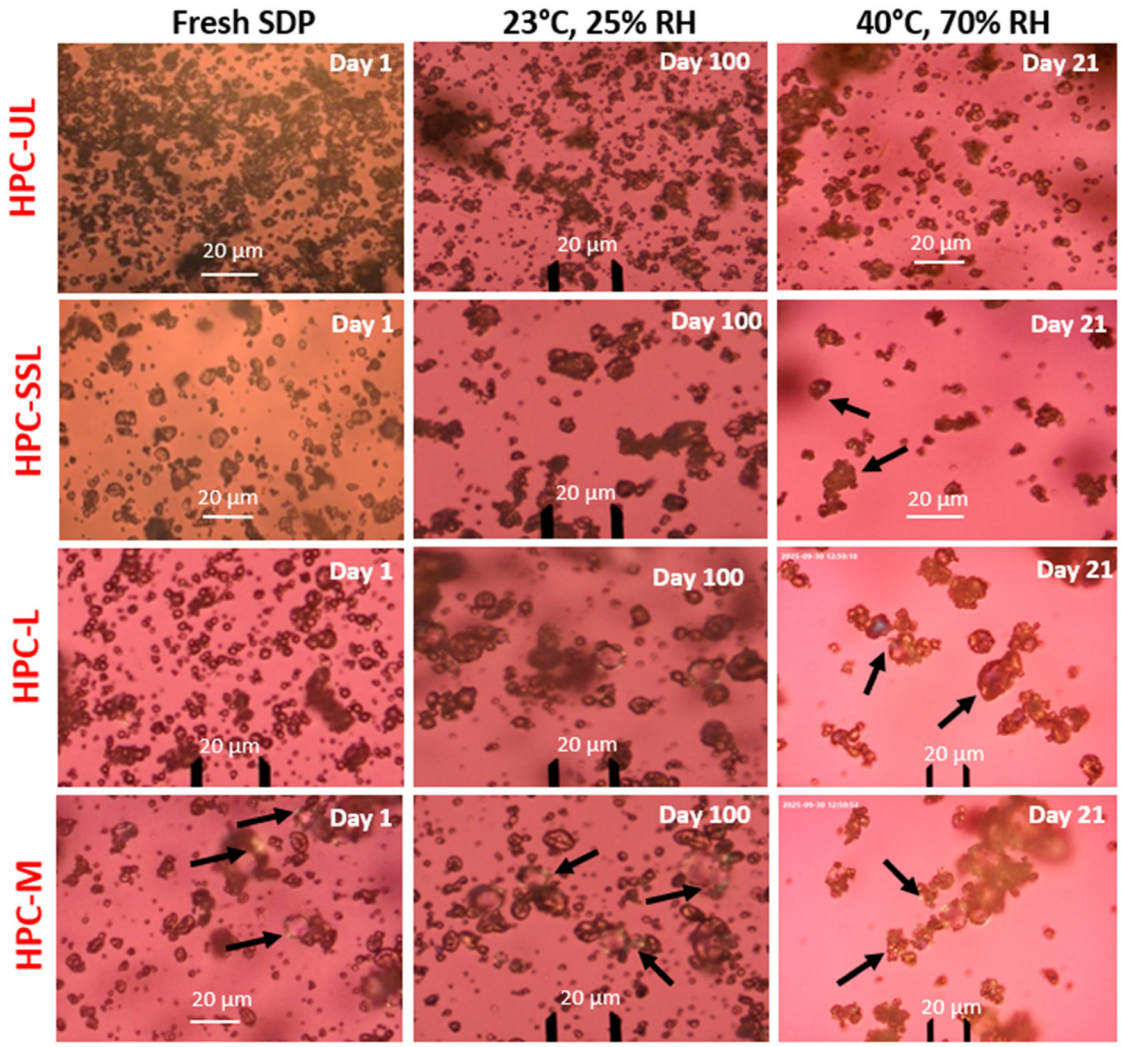

Fig. 1 PLM images of SDPs containing GLB and HPC polymers.

pronounced with SSL and much more with HPC-L and HPC-M. No signs of crystallisation were detected in the HPC-UL sample after 21 days. Upon continuing monitoring of the HPC-UL sample, PLM observations showed that the majority of the material had become birefringent after 40 days (Fig. S1).

3.1.1.2. DSC measurements. The obtained spray-dried materials (fresh SDP) were studied *via* DSC to determine their initial solid-state properties after preparation (day 1). All formulations showed visually similar thermograms with very shallow exothermic peaks around 110 °C, followed by a similarly shallow endothermic melting peak at 150–160 °C (Fig. S2 in the SI). This suggested a transition to GLB type III polymorph during the DSC heating cycle.[21] Such heat-induced crystallization during DSC can be explained by increased molecular mobility at higher temperature, which facilitates molecular rearrangement, nucleation and crystal growth. Similar behaviour has been reported previously in other studies, *e.g.* Luebbert *et al.* showed heat-induced crystallisation of itraconazole in HPC-based ASD,[8] while Mah *et al.* reported crystallisation of amorphous glibenclamide during DSC heating.[23] Duong *et al.* reported polyethylene glycol (PEG) crystallisation during DSC of indomethacin-PEG dispersion.[22]

To check whether the melting endotherm of the spray-dried materials indicates partial crystallinity after preparation (incomplete amorphisation), or it is due to heat-induced crystallisation, we determined the ratio of the heat-induced crystallisation enthalpy at 110 °C to the melting enthalpy at 150–160 °C (Table S1 in the SI). The results showed a value close to unity for the HPC-UL formulation, indicating that the material was completely amorphous and all melting was due to heat-induced crystallization. The picture for HPC-SSL and HPC-L (ratios of 0.63 and 0.71, respectively) was less clear, with data suggesting at least partial crystallinity of the initial material (*ca.* 1/3 of the melting enthalpy was not due to heat-induced crystallisation). In contrast, the heat-induced crystallisation/melting enthalpy ratio for HPC-M was 0.35, which suggests a significant crystalline fraction was already present in the initial formulation of the highest molecular weight polymer, in agreement with the PLM observations.

The DSC thermograms of the SDPs stored under ambient and accelerated conditions for 100 and 21 days, respectively, are shown in Fig. 2. Under ambient conditions (Fig. 2A), no qualitative differences could be visually observed between the thermograms obtained one day after preparation and those recorded after 100 days. The ratios of the enthalpies of heat-induced crystallisation at 110 °C and the melting enthalpy at 150–160 °C (Table S1 in the SI) confirmed no significant changes in the properties of HPC-UL, HPC-SSL and HPC-M formulations. For HPC-L, a progressive decrease in the ratio of the enthalpies suggested the accumulation of crystallised GLB during storage.

The thermograms of the SDPs stored under accelerated conditions for 21 days are presented in Fig. 2B. The samples prepared with HPC-SSL, L, and M did not exhibit exothermic peaks during heating, but showed small and broad endothermic melting peaks at approximately 150–160 °C, clearly indicating that crystallisation had occurred during storage. In contrast, HPC-UL showed a small exothermic peak and a corresponding endothermic peak, similarly to the samples stored at ambient conditions.

As the HPC-UL formulation did not show clear evidence of crystallisation after 21 days, the stability study at accelerated conditions was extended to 50 days (Fig. S3). The thermograms revealed a progressive change in the ratio between the enthalpies of heat-induced crystallisation and melting (Table S2 in the SI). At day 0, the ratio was close to unity, indicating that heat-induced crystallisation was the major source of the subsequent melting; however, the ratio gradually decreased to ≈0.5, 0.2 and finally 0 after 21, 34 and 50 days at accelerated stability conditions. This progressive shift in the heat-induced crystallisation/melting ratio can be explained by crystallisation during storage and a decreasing contribution of heat-induced crystallisation to the measured thermogram.

Modulated DSC measurements were also performed in order to determine the T_g of the spray-dried powders (Fig. S7). The measured T_g of pure amorphous GLB was around 64 °C and was consistent with the literature data, where values between 40 and 70 °C have been reported depending on the amorphisation technique.[24,25] Unfortunately, we were unable to reliably determine the T_g of the GLB-HPC formulations as no evident T_g events were noted on the thermograms. This was likely due to the very small change in heat capacity of HPC, which prevents the direct determination of T_g *via* DSC.

In summary, the DSC measurements were in line with the results from PLM: all HPC-stabilised amorphous formulations of GLB were stable even after 100 days under ambient conditions. Under accelerated conditions, signs of crystallisation were observed at the 21st day for HPC-M, L and SSL, which was consistent with the PLM data. Both DSC and PLM showed that HPC-UL provided better stability at the accelerated stability test.

3.1.1.3. WAXS measurements. The WAXS measurements (Fig. 3) were in good agreement with the PLM and DSC results. The crystalline GLB showed well-defined Bragg peaks which corresponded to GLB polymorph I (Fig. S4).[17,26] No signs of crystallinity were observed in the samples stored under ambient conditions after 100 days. Under accelerated conditions, crystallisation was confirmed in all samples by the presence of two groups of Bragg peaks at $q \approx 0.8$ and 1.4 Å^{-1}, which correspond to polymorph III of GLB.[17] Although all samples exhibited Bragg peaks, their intensity was lowest in the formulation containing HPC-UL, indicating superior stabilisation of the amorphous state of GLB. Quantitative analysis of the WAXS data was not performed as we were not able to obtain the pure type III polymorph, required for preparing a calibration curve.

The combined results from PLM, DSC, and WAXS consistently showed that incorporating HPC polymers effectively stabilised the amorphous state of GLB within the solid dispersions. Under ambient storage conditions, all formulations maintained their amorphous state for extended periods, showing no evidence of crystallisation even after several months. The stability under accelerated conditions

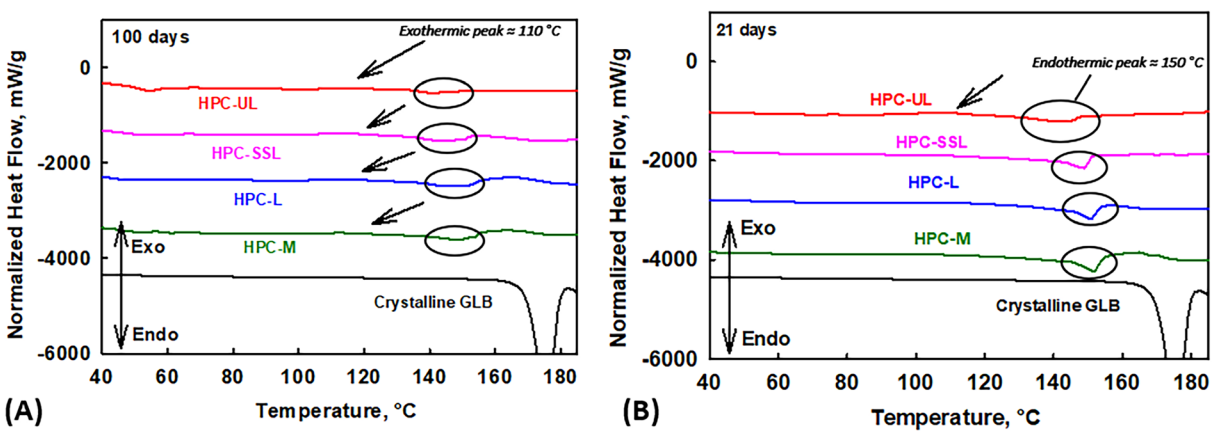

Fig. 2 DSC measurements of SDPs containing GLB and HPC polymers stored under ambient conditions (A) and accelerated conditions (B). Crystalline GLB (black); HPC-UL (red); HPC-SSL (pink); HPC-L (blue); HPC-M (green). The exothermic events are marked with black arrows and endothermic with black circles.

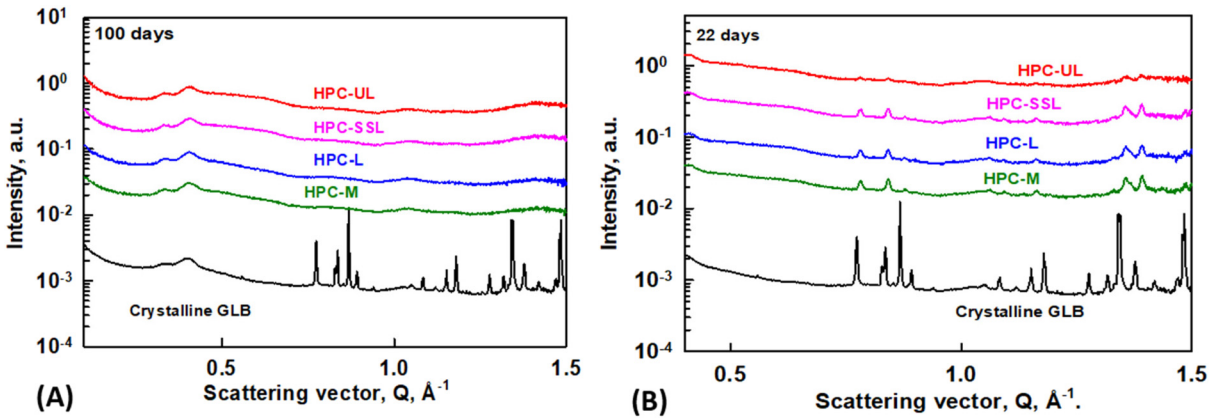

Fig. 3 WAXS measurements of SDPs containing GLB and HPC polymer stored under ambient conditions (A) and accelerated conditions (B). Crystalline GLB (black); HPC-UL (red); HPC-SSL (pink); HPC-L (blue); HPC-M (green).

was, however, affected by the molecular weight of the polymer. Crystallisation was detected with all polymers, although the onset varied across the different techniques. Despite those differences, the overall results consistently showed that the lowest-molecular-weight polymer HPC-UL provided superior solid-state stability.

3.1.2. Stability of solvent-cast films. In addition to the spray-dried powders, we studied the effect of polymer molecular weight on systems prepared by solvent casting (section 2.2.2). Both methods rely on rapid solvent evaporation to produce amorphous materials, and while spray drying is a time- and material-consuming process, solvent casting allows the preparation of amorphous films within minutes, while using a minimum quantity of material. The stability of the prepared amorphous films can be easily monitored with PLM, supporting solvent casting as a promising screening strategy for ASD preparation.[27,28]

The PLM images of the solvent-cast films stored at ambient conditions are presented in Fig. 4A.

The films prepared with SSL and UL were homogeneous throughout. Minor localised birefringence was observed in some samples; however, those regions did not grow larger with time, showing no signs of progressive crystallisation. Surface cracking during storage was noted for some of the samples but no crystalline domains were observed during the 114-day period. The films prepared with the higher molecular weight polymers L and M, however, seemed less homogeneous immediately after preparation. Certain regions in the films were reminiscent of liquid crystals although no apparent crystals or birefringence were seen in the samples. Some topographical roughness and inhomogeneity were observed, most likely caused by the higher viscosity of the casting solution. No change in the appearance was recorded as the overall morphology remained mostly unchanged throughout the entire storage period at ambient conditions.

Under accelerated conditions (T = 40 °C, RH = 70%), however, crystallisation-related processes were observed in all studied samples (Fig. 4B). The onset of crystallisation was

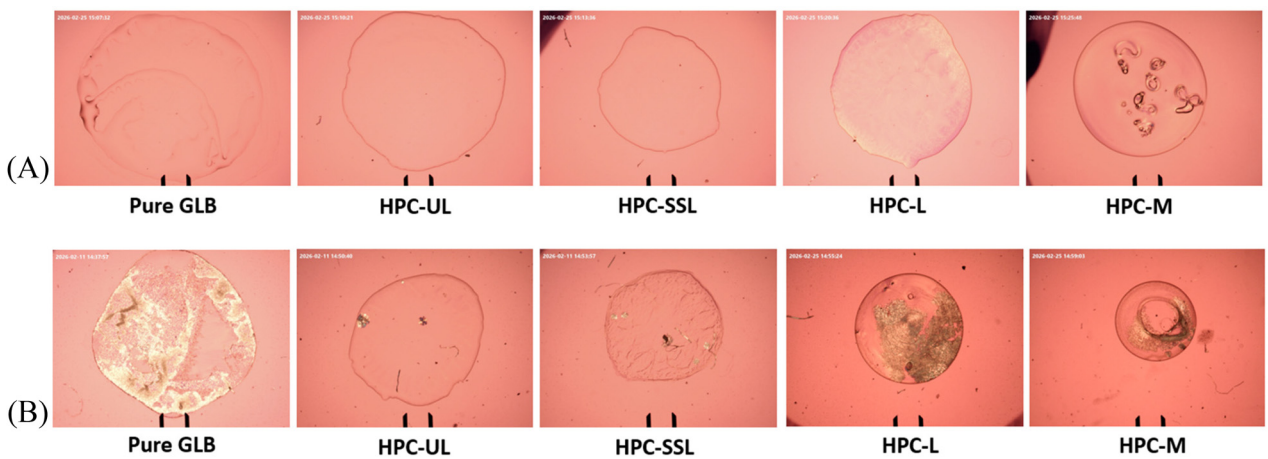

Fig. 4 Solvent-cast films of GLB with HPC polymers stored under (A) ambient conditions for 114 days or (B) accelerated conditions (T = 40 °C, RH = 70%) for 100 days. The distance between the bars is 400 μm.

defined as the time point at which the crystallised film area reaches 5% of the total film area. This threshold was selected because in some samples isolated small birefringent areas appeared early on, however, such small crystalline spots are difficult to quantify and may represent isolated local heterogeneity rather than an ongoing crystallisation process. Based on these criteria, the earliest crystallisation onset was observed with the pure GLB (20th day) followed by HPC-L (30th day) and HPC-M (40th day), whereas the HPC-UL and SSL samples did not reach the 5% crystallinity threshold.

The films with HPC-UL and SSL showed superior stability, although small visible crystals appeared on the 15th and 10th days, respectively. The crystal growth was, however, very limited as the total crystalline area never reached 5% for the entire 100-day stability experiment (Fig. 5).

In contrast, visible, well-defined crystals emerged between the 30th and 40th day for the HPC-L and HPC-M-based films. Phase separation occurred even earlier, after 2 weeks of storage, with both samples (Fig. 6). In the HPC-L samples elongated, worm-like, lamellar structures were seen under the microscope suggesting the formation of polymer-rich or drug-rich phase that preceded crystal growth. In the HPC-M sample, the phase separation differed in appearance as numerous dot-like objects appeared. Following the appearance of crystalline regions, the crystallisation process progressed steadily in both samples, reaching ≈60% on average with HPC-L, and ≈40% with HPC-M after 100 days of storage (Fig. 5).

Overall, the comparison between the two methods for studying solid-state stability (spray-dried particles *vs.* solvent-cast films) revealed some differences in the onset of crystallisation as well as its progression, but the overall trends remained in good agreement. Neither method detected crystallisation in the samples stored at ambient conditions. The experiments with samples stored under accelerated conditions consistently demonstrated the superior solid-state stability of the lower-molecular-weight polymers and HPC-UL in particular.

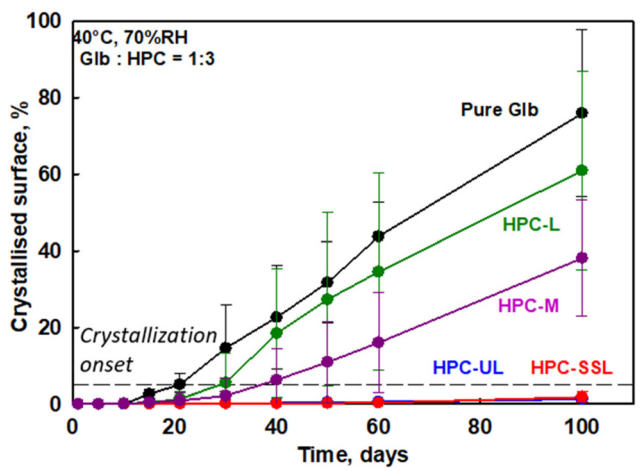

Fig. 5 Crystalline surface area of solvent-cast films of GLB and HPC as a function of time. Pure GLB (black); HPC-UL (blue); HPC-SSL (red); HPC-L (green); HPC-M (purple). The presented results are averaged from at least 3 independent samples ($n \geq 3$). Error bars can be smaller than the symbols.

3.2. Dissolution studies

The SDPs containing HPC-SSL and HPC-UL were chosen for the majority of the dissolution experiments since they showed superior solid-state stability. The limited data for HPC-L and HPC-M formulations is presented in Fig. S6 in the SI. The dissolution profiles of the spray-dried powders were studied in blank phosphate buffer (pH 6.5) and phosphate buffer (pH 6.5) containing porcine bile extract at a bile salt concentration equivalent to 3 or 10 mM, mimicking fasted and fed conditions (Fig. 7). Both formulations exhibited very similar dissolution behaviour, as rapid initial increase in GLB concentration during the first 10 min was observed, reaching approximately 100 μg mL^{-1} in blank buffer and 3 mM porcine bile. In contrast, both SDPs showed higher GLB concentrations in 10 mM porcine bile, reaching ≈160 μg mL^{-1}. Both formulations sustained this concentration for the full 120 min experiment as no precipitation was observed in any of the studied media. Dissolution experiments in porcine bile media were also conducted with HPC-L and M. The results were very similar to those obtained with the lower-molecular-weight polymers. GLB concentrations in the HPC-M system were slightly lower on average compared to the other HPC polymers, but overall, the dissolution behaviour was very similar across all studied HPC polymers (Fig. S6).

Microscopic images of the undissolved solid material were taken during dissolution to assess crystallisation (Fig. 8). In porcine bile media, no crystallisation was observed in either formulation and the material remained amorphous throughout the 120 min experiment regardless of the bile salt concentration. In pure buffer, most of the material remained amorphous after 120 min with both SDPs, with only minor crystalline regions noted under the microscope.

3.3. *In situ* rat perfusion

In situ rat perfusion experiments were conducted according to the protocols described in section 2.2.9 to evaluate the intestinal absorption of GLB from the SDPs with HPC-UL and SSL. The plasma concentration profiles and the cumulative amount of absorbed GLB are presented in Fig. 9.

The experiments were performed in 10 mM porcine bile since GLB concentrations were higher at this bile salt concentration. Both systems reached GLB concentrations of ≈170 μg mL^{-1} in the perfusate, which was in good agreement with the previous *in vitro* experiments. A rapid initial increase in plasma GLB concentrations within the first 10 min was observed with both SDPs, followed by a plateau that was maintained throughout the 60 min experiment. The measured plasma concentrations were substantially higher compared to crystalline GLB, which showed negligible absorption. The formulations containing HPC-UL and HPC-SSL exhibited very similar profiles, with steady-state plasma levels in the range of 10–20 μg mL^{-1}, indicating comparable intestinal permeability and absorption kinetics.

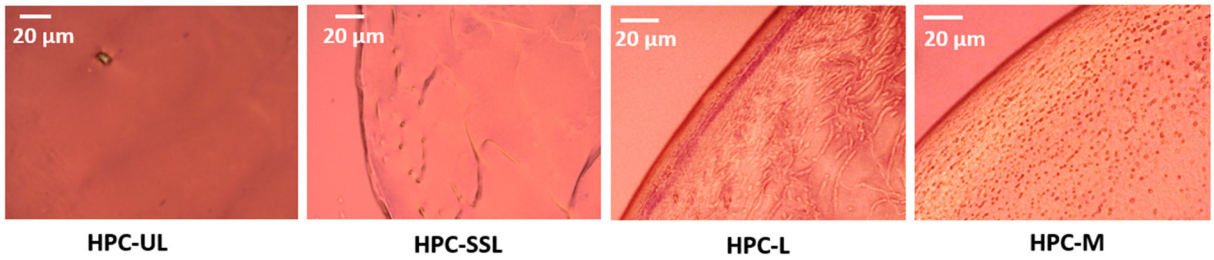

Fig. 6 Solvent-cast films of GLB and HPC polymers stored under accelerated conditions for 2 weeks.

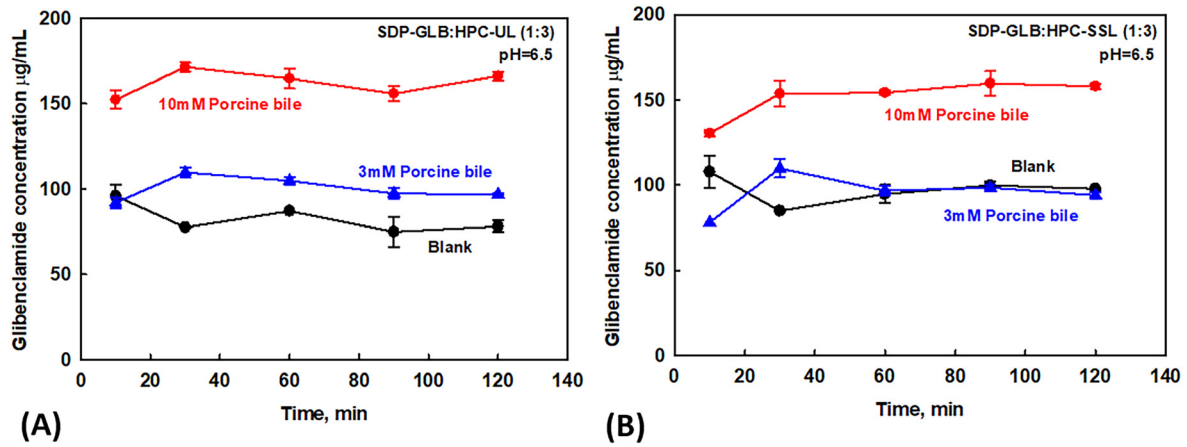

Fig. 7 Dissolution profiles of GLB-HPC ASDs in different dissolution media. GLB HPC-UL (A); GLB HPC-SSL (B). Simple phosphate buffer (black); 3 mM porcine bile media (blue); 10 mM porcine bile media (red). The presented results are averaged from at least 2 independent samples ($n \geq 2$). Error bars can be smaller than the symbols.

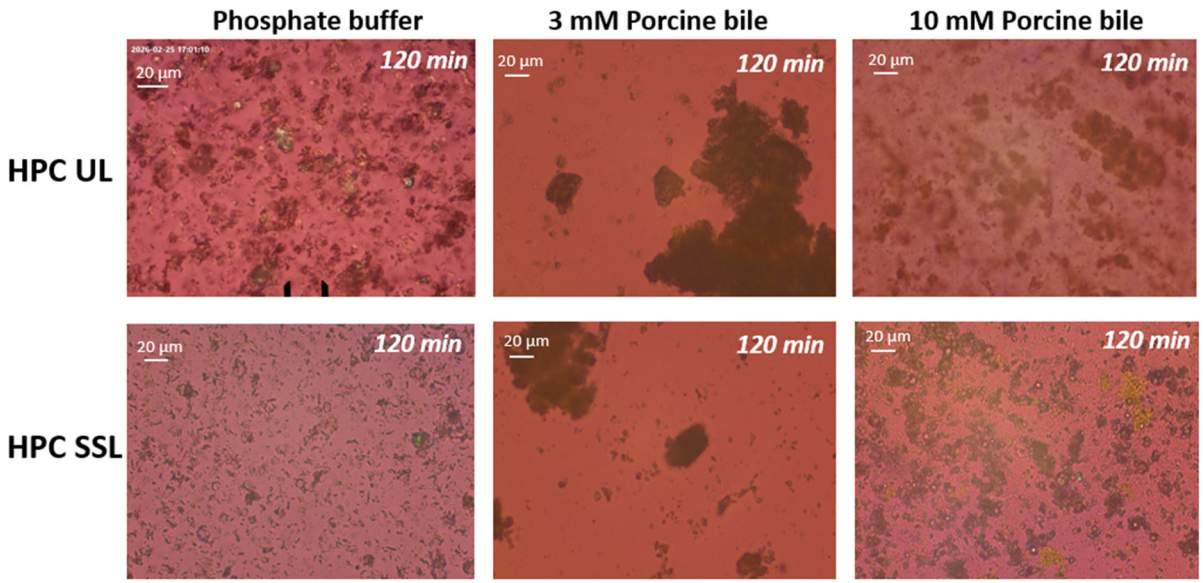

Fig. 8 PLM images of GLB material collected during dissolution of GLB-HPC ASDs in phosphate buffer pH 6.5, 3 and 10 mM porcine bile after 120 min.

The cumulative absorption data (Fig. 9B) showed a linear increase in the amount of absorbed GLB over time for both formulations. The total amount of drug absorbed after 60 min was nearly identical between the UL and SSL systems, confirming that both lower-molecular-weight HPC polymers provided efficient stabilisation for intestinal GLB supersaturation, main-

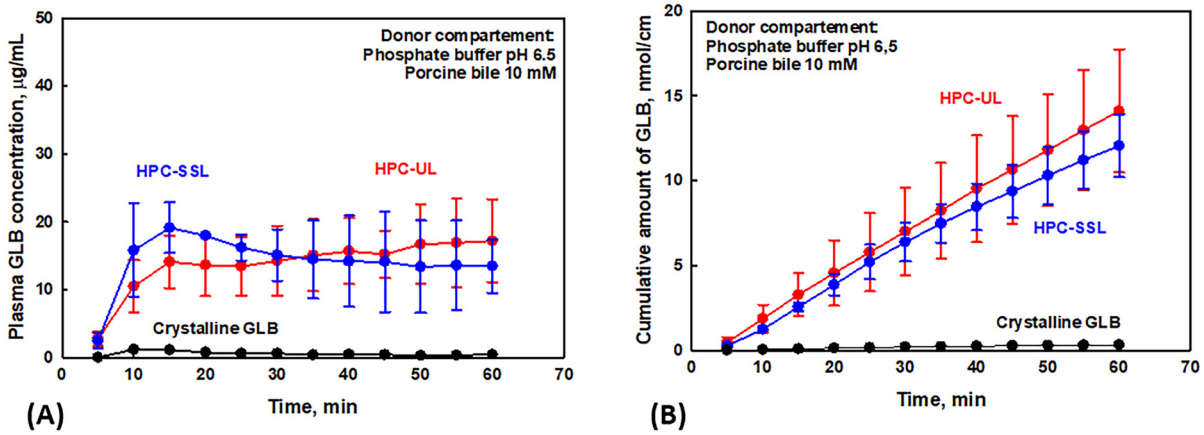

Fig. 9 GLB plasma profiles (A). Cumulative GLB absorption (B). Crystalline GLB (black); GLB HPC-UL (red); GLB HPC-SSL (blue). The presented results are averaged from at least 2 independent experiments ($n \geq 2$). Error bars can be smaller than the symbols.

taining high GLB concentrations available for absorption. In contrast, the absorption of crystalline GLB was much lower, effectively close to zero. These results demonstrate that, under biorelevant intestinal conditions containing porcine bile, both HPC-UL and SSL ASDs enhance GLB intestinal absorption to a similar degree.

4. Discussion

4.1. Effect of HPC molecular weight on solid-state stability

The solid-state stability studies conducted with SDPs and solvent-cast films showed that polymer molecular weight is an essential factor that governs long-term ASD stability. However, the effect of molecular weight could be determined only when using accelerated stability storage conditions, as no difference in the stability of the ASD stabilised by the different HPC polymers was observed after 100 days of storage at ambient conditions. Although crystallisation onset varied between the different characterisation techniques (PLM, DSC and WAXS) and between the different amorphisation techniques, the overall trend showed superior solid-state stability for the lower molecular weight polymers under accelerated conditions.

These findings are in agreement with Luebbert *et al.* who showed that lower-molecular weight HPC polymers can stabilise the amorphous form of fenofibrate more efficiently than higher molecular weight polymers at low drug loads.[8] Those findings, however, contradict what other authors have reported for other polymers, such as PVP, where the well-established paradigm states that solid-state stability and dissolution performance improves with higher molecular weight polymers.[9,10]

This conceptually different behaviour of PVP and HPC polymers suggests different mechanisms of crystallisation inhibition. The superior solid-state stability with higher M_w PVPs is mostly attributed to the lower molecular mobility, higher glass transition temperature and increased viscosity associated with the higher molecular weight PVPs.[6,11,28] A possible explanation for the superior stability with the lower molecular weight HPCs could be the higher degree of mixing between the drug and polymer molecules. Good drug–polymer miscibility is essential for the long-term stability as poor mixing promotes phase separation and crystallisation.[29] PC-SAFT data showed higher solubility of amorphous fenofibrate in lower molecular weight HPC, supporting this hypothesis.[8] Similar conclusions were reported by Pöstges *et al.*[15] The authors reported superior ASD homogeneity with the lower molecular weight HPC-UL compared to HPC-SSL.

Another contributing factor might be the viscosity of the drug–polymer solution prior to amorphisation. Lower-molecular-weight polymers produce solutions with lower viscosities, which can promote faster solvent evaporation and more homogeneous drug–polymer mixing.[30] In contrast, higher-molecular-weight polymers generate more viscous solutions which evaporate slower and may produce more heterogeneous drug–polymer mixtures that are more susceptible to phase separation and crystallisation.

HPC and PVP may also differ in terms of the specific drug–polymer interactions involved. Many authors have reported strong H-bonding interactions between PVP, a strong H-bond acceptor, and various drugs formulated into ASDs as a key stabilisation mechanism.[11,31–33] HPC, on the other hand, contains free hydroxy groups which are weak H-bond donors, but may nevertheless engage in intra- or inter-molecular H-bonding. This might diminish the potential of HPC to interact with drug molecules, hindering stabilisation. In our previous study, we conducted NMR studies of ASDs comprised of GLB and HPC-SSL where the results showed no intermolecular interactions between the drug and the polymer in the solid-state.[17] In the current study, we performed additional measurements on HPC-UL and HPC-L formulations, but also did not identify any significant interactions *via* changes in the chemical shifts (Fig. S9 and S10 in the SI). To further investigate possible differences in the molecular organization of the amorphous solids, we performed NMR relaxation measurements.

We measured the T_1 and $T_{1\rho}$ relaxation times, which probe molecular dynamics over different timescales and are sensitive to differences in the local molecular environment and mobility. The obtained results (Table S3 in the SI) showed that there are significant differences between the relaxation properties of the pure amorphous drug (T_1 = 2.3 s, $T_{1\rho}$ = 5.5 ms) and the polymers (T_1 = 1.0–1.3 s, $T_{1\rho}$ = 2.5–2.7 ms), providing sufficient resolution for characterizing the properties of the amorphous drug + polymer formulations. Such analysis showed that T_1 relaxation time of the drug shifts from 2.3 s (the value for amorphous GLB) to 1.2 s in the GLB + UL formulation, which is practically the same as the T_1 value for the pure UL polymer (1.3 s). The opposite situation was observed for the HPC-L formulation, in which the relaxation of the drug molecules retained a T_1 value similar to that of the pure amorphous drug, while their $T_{1\rho}$ (4.1 ms) was intermediate between those of the pure drug and the polymer. The obtained data supports the hypothesis of incomplete mixing and amorphous drug domains in the GLB + HPC-L formulation, in contrast to good mixing and homogeneity for the GLB + HPC-UL formulation on the T_1 lenght scale.

Martin-Pastor and Stoyanov reported hydrophobic interactions between HPC and fenofibrate both in solution and in solid state.[34] While these interactions are weaker than the H-bonds observed with PVP, the high supersaturated solution stability in the presence of low-molecular-weight HPC is driven by different mechanisms: solubilisation[35] and surface adsorption,[17] which interfere with both nucleation and crystal growth mechanisms of precipitation. The surface-active properties of low-molecular-weight HPC are supported by their less entangled[36] and more hydrophobic[37] behaviour in solution.

Overall, the better performance of lower molecular weight HPC polymers for the solid-state stability of amorphous glibenclamide appears to be driven by favourable mixing entropy, whereas the supersaturated solution stability can be linked to enhanced surface adsorption and solubilisation properties of HPC with lower molecular weight.

4.2. Dissolution, supersaturation and oral absorption

The dissolution experiments confirmed the potential of the low-molecular-weight HPCs to effectively stabilise supersaturated drug solutions. This effect was evident in the experiments in blank phosphate buffer, where both HPC-UL and SSL provided effective stabilisation against crystallisation, maintaining concentrations around 100 μg mL^{-1} throughout the experiment (Fig. 7). In contrast, when similar experiments were performed with pure amorphous GLB with no polymer, drug concentrations remained low, indicating early drug crystallisation (Fig. S5). Notably, when the HPC polymers were added to the dissolution media, GLB concentration rose to 100 μg mL^{-1}, once again confirming the ability of HPC polymers to promote and sustain supersaturation (Fig. S5).

Those findings are in good agreement with the well-established role of polymers in ASD formulations, where the polymers must provide a kinetic stabilisation for the metastable supersaturation state so that sufficient drug absorption may occur.[38,39] Other authors have also demonstrated the ability of HPC polymers to inhibit crystallisation in supersaturated solutions. In a series of studies, Niederquell *et al.* showed that HPC can be used effectively as a precipitation inhibitor, with the experimental outcome being highly dependent on factors such as drug molecule characteristics, polymer chain length, dissolution media composition and buffering media.[35,40]

In the dissolution experiments performed in porcine bile media, both formulations exhibited very similar behaviour. In the presence of 3 mM porcine bile, the dissolution profiles were identical to those in phosphate buffer, whereas in the presence of 10 mM porcine bile GLB concentrations increased to ≈160 μg mL^{-1} and were stable throughout the 120 min experiment. Increasing bile salt concentration led to enhanced GLB solubilisation, thereby resulting in even higher aqueous drug concentrations. This concentration-dependent effect of bile components is well established in the scientific literature, where the effect of bile salts and phospholipids on drug solubilisation has been extensively studied, particularly in the context of fed and fasted state intestinal fluids.[41–43]

In situ perfusion studies showed enhanced drug absorption when GLB was formulated as an ASD with HPC, compared to the crystalline drug. SDPs with both polymers once again produced very similar results, where the GLB plasma concentration and the cumulative amount of absorbed drug were essentially identical between the two polymers showing no major polymer molecular weight effect on the intestinal absorption (Fig. 9). These results are in agreement with the observations of Nihei *et al.*, who reported increased oral bioavailability of nobiletin in rats.[18] Polymer molecular weight appears to have a more pronounced effect on solid-state stability rather than intestinal absorption: once a sufficient supersaturation is generated, absorption is more likely to be governed by the aqueous drug concentrations. However, more studies with a broader range of different HPCs and larger number of animals are needed to fully confirm this hypothesis.

5. Conclusions

The solid-state stability, dissolution behaviour and intestinal absorption of GLB amorphous formulations prepared by spray drying and stabilised by four grades of HPC polymers with different molecular weight were studied. Storage under mild conditions (T = 23 °C, RH = 25%) did not discriminate between the different polymers as all formulations remained amorphous by PLM and WAXS for 100 days. Accelerated stability tests (T = 40 °C, RH = 70%) showed that solid-state stability was highest for the HPC with lower-molecular-weight, with HPC-UL having the best performance overall. Good agreement was observed between the stability studies performed with spray-dried powders and solvent-cast films, suggesting that solvent casting can be used as a quick and flexible method for stability screening. The superior solid-state stability provided by the lower-molecular-weight HPCs was attributed to improved drug–polymer mixing as illustrated by NMR relaxo-

metry and amorphous film imaging. The low-molecular-weight HPC-SSL and HPC-UL showed very good supersaturation stability and markedly increased the intestinal drug absorption during *in situ* rat perfusion, compared to the crystalline drug reference. The study revealed the significant impact of HPC molecular weight on solid-state stability of high-drug-load ASDs prepared by spray drying, as well as a substantial increase in intestinal drug absorption when formulated as ASD with low-molecular-weight HPC polymers.

Conflicts of interest

E. Stoyanov is an employee of Nisso Chemical Europe GmbH, which manufactures the HPC grades studied in this work and provided the samples. The other authors declare no conflicts of interest.

Data availability

Data for this article, including the raw data for all figures in the main text are available at Zenodo at https://doi.org/10.5281/zenodo.20795681.

Supplementary information (SI) is available. See DOI: https://doi.org/10.1039/d6pm00307a.

Acknowledgements

Z. V. gratefully acknowledges the support of the Bulgarian Ministry of Education and Science and the Bulgarian National Science Fund under the National Research Program "VIHREN-2021", project 3D-GUT (No. KP-06-DV-3/15.12.2021).

References

1 L. S. Taylor and G. G. Z. Zhang, Physical chemistry of supersaturated solutions and implications for oral absorption, *Adv. Drug Delivery Rev.*, 2016, **101**, 122–142, DOI: 10.1016/j.addr.2016.03.006.

2 G. A. Ilevbare and L. S. Taylor, Liquid–liquid phase separation in highly supersaturated aqueous solutions of poorly water-soluble drugs: implications for solubility-enhancing formulations, *Cryst. Growth Des.*, 2013, **13**, 1497–1509, DOI: 10.1021/cg301679h.

3 V. Wilson, X. Lou, D. J. Osterling, D. F. Stolarik, G. Jenkins, W. Gao, G. G. Z. Zhang and L. S. Taylor, Relationship between amorphous solid dispersion in vivo absorption and in vitro dissolution: phase behavior during dissolution, speciation, and membrane mass transport, *J. Controlled Release*, 2018, **292**, 172–182, DOI: 10.1016/j.jconrel.2018.11.003.

4 S. V. Bhujbal, B. Mitra, U. Jain, Y. Gong, A. Agrawal, S. Karki, L. S. Taylor, S. Kumar and Q. T. Zhou, Pharmaceutical amorphous solid dispersion: a review of manufacturing strategies, *Acta Pharm. Sin. B*, 2021, **11**, 2505–2536, DOI: 10.1016/j.apsb.2021.05.014.

5 K. Ueda, D. E. Moseson and L. S. Taylor, Amorphous solubility advantage: theoretical considerations, experimental methods, and contemporary relevance, *J. Pharm. Sci.*, 2025, **114**, 18–39, DOI: 10.1016/j.xphs.2024.08.029.

6 S. Mohapatra, S. Samanta, K. Kothari, P. Mistry and R. Suryanarayanan, Effect of polymer molecular weight on the crystallization behavior of indomethacin amorphous solid dispersions, *Cryst. Growth Des.*, 2017, **17**, 3142–3150, DOI: 10.1021/acs.cgd.7b00096.

7 N. Li and L. S. Taylor, Tailoring supersaturation from amorphous solid dispersions, *J. Controlled Release*, 2018, **279**, 114–125, DOI: 10.1016/j.jconrel.2018.04.014.

8 C. Luebbert, E. Stoyanov and G. Sadowski, Phase behavior of ASDs based on hydroxypropyl cellulose, *Int. J. Pharm.: X*, 2021, **3**, 100070, DOI: 10.1016/j.ijpx.2020.100070.

9 U. S. Kestur, H. Lee, D. Santiago, C. Rinaldi, Y. Y. Won and L. S. Taylor, Effects of the molecular weight and concentration of polymer additives, and temperature on the melt crystallization kinetics of a small drug molecule, *Cryst. Growth Des.*, 2010, **10**, 3585–3595, DOI: 10.1021/cg1004853.

10 M. M. Knopp, N. E. Olesen, P. Holm, P. Langguth, R. Holm and T. Rades, Influence of polymer molecular weight on drug–polymer solubility: a comparison between experimentally determined solubility in PVP and prediction derived from solubility in monomer, *J. Pharm. Sci.*, 2015, **104**, 2905–2912, DOI: 10.1002/jps.24410.

11 J. Zhang, M. Guo, M. Luo and T. Cai, Advances in the development of amorphous solid dispersions: the role of polymeric carriers, *Asian J. Pharm. Sci.*, 2023, **18**, 100834, DOI: 10.1016/j.ajps.2023.100834.

12 J. Brady, T. Dürig, P. I. Lee and J. X. Li, Polymer properties and characterization, in *Developing Solid Oral Dosage Forms: Pharmaceutical Theory and Practice*, ed. Y. Qiu, Y. Chen, G. G. Z. Zhang, L. Yu and R. V. Mantri, Academic Press, 2nd edn, 2017, pp. 181–223. DOI: 10.1016/B978-0-12-802447-8.00007-8.

13 A. L. Sarode, S. A. Malekar, C. Cote and D. R. Worthen, Hydroxypropyl cellulose stabilizes amorphous solid dispersions of the poorly water-soluble drug felodipine, *Carbohydr. Polym.*, 2014, **112**, 512–519, DOI: 10.1016/j.carbpol.2014.06.039.

14 F. Pöstges, K. Kayser, E. Stoyanov and K. G. Wagner, Boost of solubility and supersaturation of celecoxib via synergistic interactions of methacrylic acid–ethyl acrylate copolymer (1 : 1) and hydroxypropyl cellulose in ternary amorphous solid dispersions, *Int. J. Pharm.: X*, 2022, **4**, 100115, DOI: 10.1016/j.ijpx.2022.100115.

15 F. Pöstges, J. Lenhart, E. Stoyanov, D. J. Lunter and K. G. Wagner, Phase homogeneity in ternary amorphous solid dispersions and its impact on solubility, dissolution and supersaturation—Influence of processing and hydroxypropyl cellulose grade, *Int. J. Pharm.: X*, 2023, **6**, 100222, DOI: 10.1016/j.ijpx.2023.100222.

16 N. N. S. Mai, Y. Otsuka, S. Goto, Y. Kawano and T. Hanawa, Effects of polymer molecular weight on curcumin amorphous solid dispersion: at-line monitoring system based on attenuated total reflectance mid-infrared and near-infrared spectroscopy, *J. Drug Delivery Sci. Technol.*, 2021, **61**, 102278, DOI: 10.1016/j.jddst.2020.102278.
17 V. Petkov, Z. Vinarov and S. Tcholakova, Mechanisms of dissolution and crystallization of amorphous glibenclamide, *Int. J. Pharm.*, 2024, **666**, 124820, DOI: 10.1016/j.ijpharm.2024.124820.
18 T. Nihei, E. Ushiro, H. Sato and S. Onoue, Biopharmaceutical study on nobiletin-loaded amorphous solid dispersion with improved hypouricemic effect, *Molecules*, 2021, **26**(15), 4447, DOI: 10.3390/molecules26154447.
19 R. D. Bachmaier, M. Monschke, T. Faber, A. K. Krome, Y. Pellequer, E. Stoyanov, A. Lamprecht and K. G. Wagner, In vitro and in vivo assessment of hydroxypropyl cellulose as functional additive for enabling formulations containing itraconazole, *Int. J. Pharm.: X*, 2021, **3**, 100076, DOI: 10.1016/j.ijpx.2021.100076.
20 J. Stappaerts, J. Brouwers, P. Annaert and P. Augustijns, In situ perfusion in rodents to explore intestinal drug absorption: challenges and opportunities, *Int. J. Pharm.*, 2015, **478**, 665–681, DOI: 10.1016/j.ijpharm.2014.11.035.
21 M. A. Hassan, M. Sheikh Salem, E. Sallam and M. K. Al-Hindawi, Preparation and characterization of a new polymorphic form and a solvate of glibenclamide, *Acta Pharm. Hung.*, 1997, **67**, 81–88.
22 T. V. Duong, J. Van Humbeeck and G. Van den Mooter, Crystallization kinetics of indomethacin/polyethylene glycol dispersions containing high drug loadings, *Mol. Pharm.*, 2015, **12**, 2493–2504, DOI: 10.1021/acs.molpharmaceut.5b00299.
23 P. T. Mah, T. Laaksonen, T. Rades, J. Aaltonen, L. Peltonen and C. J. Strachan, Unravelling the relationship between degree of disorder and the dissolution behavior of milled glibenclamide, *Mol. Pharm.*, 2014, **11**, 234–242, DOI: 10.1021/mp4004145.
24 Z. Wojnarowska, K. Grzybowska, K. Adrjanowicz, K. Kaminski, M. Paluch, L. Hawelek, R. Wrzalik, M. Dulski, W. Sawicki, J. Mazgalski, A. Tukalska and T. Bieg, Study of the amorphous glibenclamide drug: analysis of the molecular dynamics of quenched and cryomilled material, *Mol. Pharm.*, 2010, **7**, 1692–1707, DOI: 10.1021/mp100077c.
25 S. Rehder, A. Sakmann, T. Rades and C. S. Leopold, Thermal degradation of amorphous glibenclamide, *Eur. J. Pharm. Biopharm.*, 2012, **80**, 203–208, DOI: 10.1016/j.ejpb.2011.07.009.
26 A. Panagopoulou-Kaplani and S. Malamataris, Preparation and characterisation of a new insoluble polymorphic form of glibenclamide, *Int. J. Pharm.*, 2000, **195**, 239–246, DOI: 10.1016/S0378-5173(99)00401-9.
27 M. T. Davis, D. P. Egan, M. Kuhs, A. B. Albadarin, C. S. Griffin, J. A. Collins and G. M. Walker, Amorphous solid dispersions of BCS class II drugs: a rational approach to solvent and polymer selection, *Chem. Eng. Res. Des.*, 2016, **110**, 192–199, DOI: 10.1016/j.cherd.2016.04.008.
28 E. Browne, Z. A. Worku and A. M. Healy, Physicochemical properties of poly-vinyl polymers and their influence on ketoprofen amorphous solid dispersion performance: a polymer selection case study, *Pharmaceutics*, 2020, **12**(5), 433, DOI: 10.3390/pharmaceutics12050433.
29 J. A. Baird and L. S. Taylor, Evaluation of amorphous solid dispersion properties using thermal analysis techniques, *Adv. Drug Delivery Rev.*, 2012, **64**, 396–421, DOI: 10.1016/j.addr.2011.07.009.
30 A. Singh and G. Van den Mooter, Spray drying formulation of amorphous solid dispersions, *Adv. Drug Delivery Rev.*, 2016, **100**, 27–50, DOI: 10.1016/j.addr.2015.12.010.
31 L. S. Taylor and G. Zografi, Spectroscopic characterization of interactions between PVP and indomethacin in amorphous molecular dispersions, *Pharm. Res.*, 1997, **14**, 1691–1698, DOI: 10.1023/A:1012167410376.
32 M. Li, F. Meng, Y. Tsutsumi, J. P. Amoureux, W. Xu, X. Lu, F. Zhang and Y. Su, Understanding molecular interactions in rafoxanide–povidone amorphous solid dispersions from ultrafast magic angle spinning NMR, *Mol. Pharm.*, 2020, **17**, 2196–2207, DOI: 10.1021/acs.molpharmaceut.0c00317.
33 K. Kothari, V. Ragoonanan and R. Suryanarayanan, The role of drug–polymer hydrogen-bonding interactions on the molecular mobility and physical stability of nifedipine solid dispersions, *Mol. Pharm.*, 2015, **12**, 162–170, DOI: 10.1021/mp5005146.
34 M. Martin-Pastor and E. Stoyanov, New insights into the use of hydroxypropyl cellulose for drug solubility enhancement: an analytical study of sub-molecular interactions with fenofibrate in solid state and aqueous solutions, *J. Polym. Sci.*, 2021, **59**, 1855–1865, DOI: 10.1002/pol.20210240.
35 A. Niederquell, E. Stoyanov and M. Kuentz, Hydroxypropyl cellulose for drug precipitation inhibition: from the potential of molecular interactions to performance considering microrheology, *Mol. Pharm.*, 2022, **19**, 690–703, DOI: 10.1021/acs.molpharmaceut.1c00832.
36 M. Yoshida, H. Iwase, Y. Horikawa and T. Shikata, Evidence of a rod-like structure for hydroxypropyl cellulose samples in aqueous solution, *Biomacromolecules*, 2024, **25**, 4255–4266, DOI: 10.1021/acs.biomac.4c00334.
37 M. Martin-Pastor and E. Stoyanov, Mechanism of interaction between hydroxypropyl cellulose and water in aqueous solutions: importance of polymer chain length, *J. Polym. Sci.*, 2020, **58**, 1632–1641, DOI: 10.1002/pol.20200185.
38 J. Brouwers, M. E. Brewster and P. Augustijns, Supersaturating drug delivery systems: the answer to solubility-limited oral bioavailability?, *J. Pharm. Sci.*, 2009, **98**, 2549–2572, DOI: 10.1002/jps.21650.
39 H. R. Guzmán, M. Tawa, Z. Zhang, P. Ratanabanangkoon, P. Shaw, C. R. Gardner, H. Chen, J. P. Moreau, Ö. Almarsson and J. F. Remenar, Combined use of crystalline salt forms and precipitation inhibitors to improve oral

absorption of celecoxib from solid oral formulations, *J. Pharm. Sci.*, 2007, **96**, 2686–2702, DOI: 10.1002/jps.20906.

40 A. Niederquell, E. Stoyanov and M. Kuentz, Physiological buffer effects in drug supersaturation—a mechanistic study of hydroxypropyl cellulose as precipitation inhibitor, *J. Pharm. Sci.*, 2023, **112**, 1897–1907, DOI: 10.1016/j.xphs.2023.02.013.

41 J. H. Fagerberg, O. Tsinman, N. Sun, K. Tsinman, A. Avdeef and C. A. S. Bergström, Dissolution rate and apparent solubility of poorly soluble drugs in biorelevant dissolution media, *Mol. Pharm.*, 2010, **7**, 1419–1430, DOI: 10.1021/mp100049m.

42 C. M. Madsen, K. I. Feng, A. Leithead, N. Canfield, S. A. Jørgensen, A. Müllertz and T. Rades, Effect of composition of simulated intestinal media on the solubility of poorly soluble compounds investigated by design of experiments, *Eur. J. Pharm. Sci.*, 2018, **111**, 311–319, DOI: 10.1016/j.ejps.2017.10.003.

43 P. Augustijns, B. Wuyts, B. Hens, P. Annaert, J. Butler and J. Brouwers, A review of drug solubility in human intestinal fluids: implications for the prediction of oral absorption, *Eur. J. Pharm. Sci.*, 2014, **57**, 322–332, DOI: 10.1016/j.ejps.2013.08.027.